Transactions of the Korean Nuclear Society Virtual Spring Meeting
July 9-10, 2020

Modeling of In-Vessel Gap Cooling and Validation against LAVA, ALPHA, and LMP200 Experiments

Moon Won Song [a], Dongyeol Yeo [b] ,Hee Cheon NO [a*]
[a]*Korea Advanced Institute of Science and Technology (KAIST), Department of Nuclear and Quantum Engineering, 291, Daehak-ro, Yuseong-gu, Daejeon, 34141, Republic of Korea*
[b]*University of Michigan-Ahn Arobr, Department of Nuclear Engineering and Radiological Sciences, 2355, Bonisteel Boulevard, Ann Arbor, Michigan, U.S.A. 48109*
[*]*Corresponding author: hcno@kaist.ac.kr*

1. Introduction

From cleanup study of the TMI-2 accident, it was found that the water penetration through gap between the melt and the vessel continuously cooled down the reactor vessel [1]. Thus, several experiments and modeling of gap cooling were carried out. There are two types for existing gap cooling analysis; steady analysis and transient analysis.

The steady analysis compares the heat transfer rate from a melt with heat removal rate by the gap cooling. It is simple to evaluate whether the vessel fails or not. However, the gap thickness changes with time due to the thermal deformations of the melt and the vessel. Thus, the maximum heat removal rate through the gap change because of the change of the gap thickness. Moreover, the thermal behavior of the vessel is necessary to figure out the vessel failure mechanism, but the steady analysis cannot get the thermal trend of one.

Existing transient gap cooling analysis were developed with consideration of the thermal behavior of the melt and the vessel. These are LILAC-meltpool code (KAERI, 2002), CAMP code (JAERI, 2003), Okano's study (INSS, 2003, 2005), and SAMPSON code (Tokyo Tech, 2008). These codes well predicted the experimental data, but it has some limitations to implement to actual reactor condition as follows; no plausible mechanism of gap formation, too high cost to implement to the existing severe accident code, the lack of study on melt mass scale.

This study developed a transient gap cooling analysis which predicts the thermal behavior of a melt, a crust, a gap, and a vessel with the gap formation mechanism considering the interaction between the melt and the water. In order to reduce the calculation cost, dimension of the vessel was one-dimensional, and it was shown that the one-dimensional calculation can be sufficiently substituted for two-dimensional one. Moreover, the study on mass scale was conducted with LAVA, ALPHA, and LMP200 experiments.

2. Modeling of Gap Cooling

Fig. 1 and 2 shows the geometries and procedure to analyze the gap cooling phenomenon. In the initial phase, discretization, setting properties and constitutive parameters are carried out. The initial gap thickness can be obtained based on the calculation of Inverse Leidenfrost effect (Eq. (1)).

$$\delta_{gap,initial} = 0.464C\frac{k_{g,eff}^{\;3/8}\Delta T^{3/8}\mu_g^{\;1/24}}{(mg)^{5/24}\rho_g^{\;5/24}h_{fg}^{\;3/8}}R$$

where

$$k_{g,eff} = \frac{\delta}{D_h}k_g Nu + \varepsilon\sigma\left(T_d^{\;2}+T_w^{\;2}\right)\left(T_d+T_w\right)\delta \qquad (1)$$

$$C = \left(\int_0^{\theta_0}\sin\theta\left(\int_0^{\theta}\left(\frac{1-\cos\theta'}{\sin\theta'}\right)^{9/5}d\theta'\right)d\theta\right)^{5/24}$$

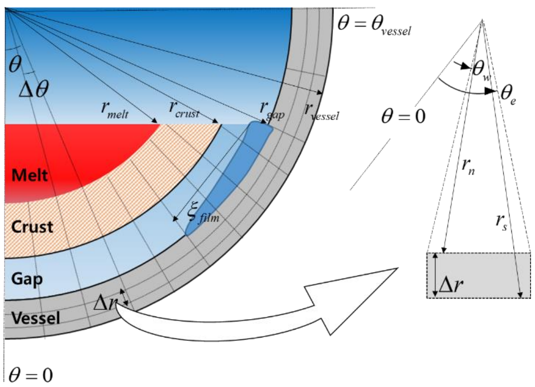

Fig. 1. Geometries of melt, crust, gap, and vessel

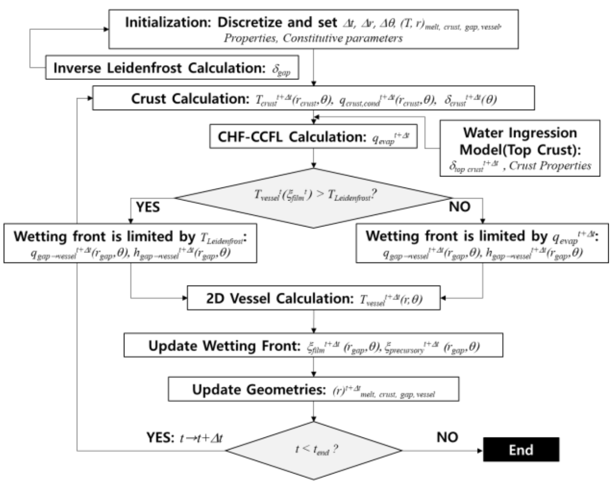

Fig. 2. Calculation procedure for gap cooling analysis

After then, the crust calculation is conducted to get the crust temperature and heat transfer rate from the crust outer surface. There are two regions on the crust outer surface, one region is in front of water front, and another is behind the water front. The heat transfer modes differs according to each region as follows;

On the region behind the water front:

$$\dot{q}_{cond,crust} = \dot{q}_{rad} + \dot{q}_{cond,gap} = \dot{q}_{gap\rightarrow vessel} \tag{2}$$

$$\begin{aligned} &\rightarrow \frac{k_{crust} dA_{r=r_{crust}}}{r_{crust}^{2}\left[\left(1/r_{melt} - 1/r_{crust}\right)\right]}\left(T_{melt,mp} - T_{crust}^{t_0+\Delta t}\right) \\ &= \sigma\varepsilon dA_{r=r_{crust}}\left(\left(T_{crust}^{t_0+\Delta t}\right)^4 - T_{vessel}^{t_0}(\theta)^4\right) \\ &+ \frac{k_{vapor} dA_{r=r_{crust}}}{r_{crust}^{2}\left[\left(1/r_{crust} - 1/r_{gap}\right)\right]}\left(T_{crust}^{t_0+\Delta t} - T_{vessel}^{t_0}(\theta)\right) \end{aligned} \tag{3}$$

On the region in front of the water front:

$$\dot{q}_{cond,crust} = \dot{q}_{rad} + \dot{q}_{fb,gap} \tag{4}$$

$$\begin{aligned} &\rightarrow \frac{k_{crust} dA_{r=r_{crust}}}{r_{crust}^{2}\left[\left(1/r_{melt} - 1/r_{crust}\right)\right]}\left(T_{melt,mp} - T_{crust}^{t_0+\Delta t}\right) \\ &= \sigma\varepsilon dA_{r=r_{crust}}\left(\left(T_{crust}^{t_0+\Delta t}\right)^4 - T_{sat}^{4}\right) \\ &+ \frac{Nuk_{vapor} dA_{r=r_{crust}}}{r_{crust}^{2}\left[\left(1/r_{crust} - 1/r_{gap}\right)\right]}\left(T_{crust}^{t_0+\Delta t} - T_{sat}\right) \end{aligned} \tag{5}$$

Through the above calculations, the temperature of the crust outer surface and the heat flux were obtained.

$$\begin{aligned} &\rho_{melt} A_{r=r_{melt}} h_{fs} \frac{\Delta\delta_{crust}}{\Delta t} \\ &= \frac{k_{crust} A_{r=r_{melt}}}{r_{melt}^{2}\left[\left(1/r_{melt} - 1/r_{crust}\right)\right]}\left(T_{melt,mp} - T_{crust}^{t_0+\Delta t}\right) \end{aligned} \tag{6}$$

Afterward, the total heat removal rate by evaporation of the penetrating water is evaluated. The heat removal rate is calculated by multiplying the penetrating water flow rate to the phase change heat. The water flow rate is calculated using the mass balance due to the phase change (Eq. (8)) and the flooding correlation [2].

$$q''_{evap} = \rho_g j_g h_{fg} \frac{A_{flow}}{A_{heater}} \tag{7}$$

$$\rho_f j_f = \rho_g j_g \tag{8}$$

$$\left(\frac{j_g}{\alpha} + \frac{j_f}{1-\alpha}\right)^2 = \left(\Delta\rho g w\right)\left(\frac{\alpha}{\rho_g} + \frac{1-\alpha}{\rho_f}\right) \tag{9}$$

$$\alpha_f = 1.06\, j_f^{*\,0.137} \tag{10}$$

The next step is to calculate the thermal behavior of the vessel by solving the heat conduction equation as below

$$\begin{aligned} \rho c_p \frac{\partial T}{\partial t}\Delta V &= k_e \left.\frac{\partial T}{r\partial\theta}\right|_e \Delta A_e - k_w \left.\frac{\partial T}{r\partial\theta}\right|_w \Delta A_w \\ &+ k_n \left.\frac{\partial T}{\partial r}\right|_n \Delta A_n - k_s \left.\frac{\partial T}{\partial r}\right|_s \Delta A_s \end{aligned} \tag{11}$$

where

$$\Delta V = \frac{2}{3}\pi\left(r_o^3 - r_i^3\right)\left(\cos\theta_w - \cos\theta_e\right) \tag{12}$$

$$\Delta A_e = \pi\sin\theta_e\left(r_s^2 - r_n^2\right) \tag{13}$$

$$\Delta A_w = \pi\sin\theta_w\left(r_s^2 - r_n^2\right) \tag{14}$$

$$\Delta A_s = 2\pi r_s^2\left(\cos\theta_w - \cos\theta_e\right) \tag{15}$$

$$\Delta A_n = 2\pi r_n^2\left(\cos\theta_w - \cos\theta_e\right) \tag{16}$$

with B.C.s

$$\text{on } (r,\theta) = (r,0);\ \left.\frac{\partial T}{r\partial\theta}\right|_w = 0 \text{ (symmetric)} \tag{17}$$

$$\text{on } (r,\theta) = (r,\theta_{vessel});\ T = T_{initial} \tag{18}$$

$$\begin{aligned} &\text{on } (r,\theta) = (r_{gap},\theta); \\ &-k_n \left.\frac{\partial T}{\partial\theta}\right|_n = q''_{gap\rightarrow vessel} - h(T_{vessel} - T_{sat}) \end{aligned} \tag{19}$$

$$\text{on } (r,\theta) = (r_{vessel},\theta);\ -k_s \left.\frac{\partial T}{\partial\theta}\right|_s = \varepsilon\sigma\left(T_{vessel}^4 - T_\infty^4\right) \tag{20}$$

Eq. (19), the heat boundary condition in the gap, is the most important condition to govern the thermal behavior of the vessel. The h, $q''_{gap\text{->}vessel}$ on Eq. (19) were determined as Table I.

This study proposed two idea for identification of the water front location. One is that the water front location can be found by heat balance as expressed in Eq. (21) when the temperature of the water front location is lower than the Leidenfrost temperature, $T_{Leidenfrost}$. Another is that the temperature of the water front location can not exceed the Leidenfrost temperature. But in this case, the penetrating water may not be completely evaporated. For the complete evaporation of the penetrating water, the over flow is allowed beyond the water front. The over flow region was named precursory region. The precursory region can be found using the heat balance, Eq. (22).

$$\dot{q}_{evap} = \sum_{wetted}\dot{q}_{crust,rad} + \sum_{wetted}\dot{q}_{vessel} \tag{21}$$

$$\begin{aligned} \dot{q}_{evap} &= \sum_{wetted}\dot{q}_{crust,rad} + \sum_{wetted}\dot{q}_{vessel,conv} \\ &+ \sum_{precursory}\dot{q}_{vessel,pre} + \sum_{precursory}\dot{q}_{crust,rad} \end{aligned} \tag{22}$$

Table I. Heat boundary conditions according to region of the vessel inner surface

	Wetting Region		Location of Water Front	Precursory Region		Location of Precursory Front	Dried Region	
	h	q''		h	q''		h	q''
No Over flow ($T_{waterfront} < T_{Leidenfrost}$)	h_{wetted}	0	Eq. (21)	No precursory region		No precursory region	0	$q''_{crust,\ rad}$
Over flow in front of the water front ($T_{waterfront} = T_{Leidenfrost}$)	h_{wetted}	0	Location of $T = T_{Leidenfrost}$	h_{film}	0	Eq. (22)	0	$q''_{crust,\ rad}$

The next step is to update the geometries considering the crust shrinkage, the vessel thermal expansion, the fracture of the crust as follows;

$$\delta_{gap}{}^{i} = \delta_{Inv\_Leidenfrost} + \delta_{th\_contraction}{}^{i} - \delta_{th\_fracture}{}^{i} \tag{23}$$

where the $\delta_{th\_fracture}$ can be obtained by these relations.

$$\frac{E_c \beta_c \left[T_{sol} - T_{crust\_front}\right]}{1-\nu_c} > \sigma_{TS} \tag{24}$$

$$\frac{E_c s^2}{1-\nu_c} \int_0^{d_c} \beta_c^2 \left(T_{sol} - T_{crust}(x)\right)^2 dx \geq 2 G_c s d_c \tag{25}$$

$$g_i = s_i \beta_c \left[T(0) - T_{sat}\right] \tag{26}$$

$$\delta_{th\_fracture}{}^{i} = \left(\frac{l_i}{s_i} - 1\right) g_i \tag{27}$$

To calculate the procedure of the gap cooling analysis, several constitutive parameters are necessary as belows;

- $T_{Leidenfrost} = T_{sat} + 100$ (K)
- $h_{wetted} = 8{,}000$ W/m^2.K
- h_{film} Bromely correlation
- Bottom heat enhancement facter: 8 on θ < 10 Deg.

3. Results and Sensitivity Studies

Table II and Fig. 3 show the gap cooling experiments for the validation and results, respectively. As can be seen, the peak temperature and the time on the peak are comparable with experimental data except the ALPHA-IDC002 case. The dimension of the vessel was one-dimensional along the altitudinal direction.

Table II. Experiments for validation of gap cooling analysis

	Melt Mass	Vessel Radius& Thickness	Pressure	Sub-cooling	Water level
LAVA-4 (reference)	30kg	0.25m, 0.025m	17.9bar	50K	50cm
ALPHA-IDC001	30kg	0.25m, 0.025m	13.0bar	20K	30cm
ALPHA-IDC002	50kg	0.25m, 0.025m	13.0bar	15K	50cm
LAVA-11	70kg	0.25m, 0.025m	17.3bar	52K	60cm
LMP200-2	200kg	0.40m, 0.040m	14.2bar	50K	60cm

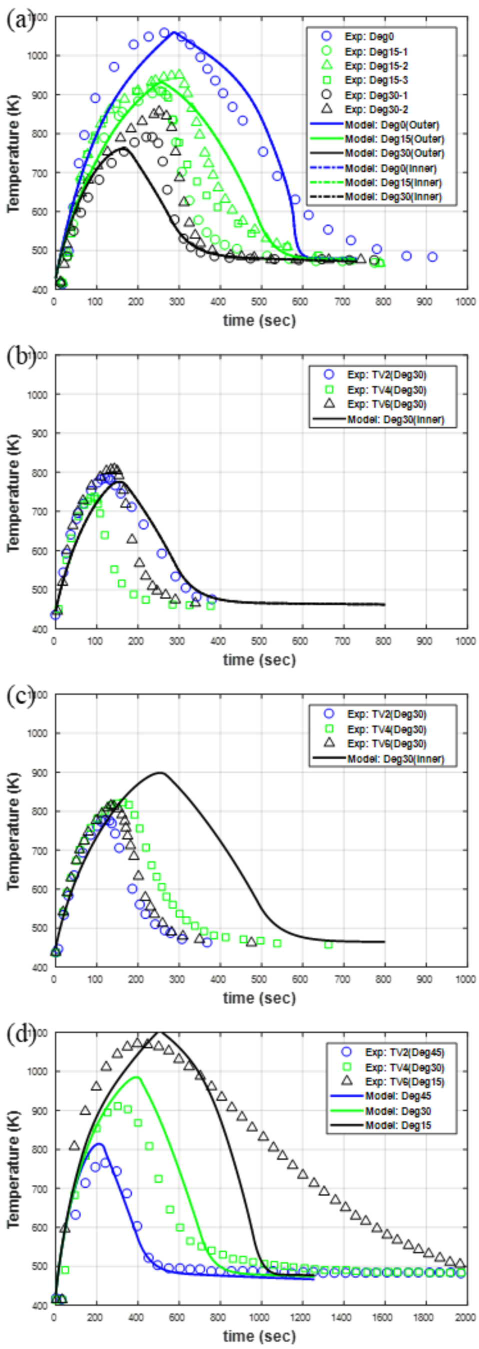

Fig. 3. Calculation results and comparison with experiments (a): LAVA-4, (b): ALPHA-IDC001, (c): ALPHA-IDC002, (d): LAVA-11

Fig. 4 shows the sensitivity study for the dimension of the vessel. As illustrate on Fig. 4, one-dimensional calculation is enough to substitute the two-dimensional one, so it can reduce the calculation cost.

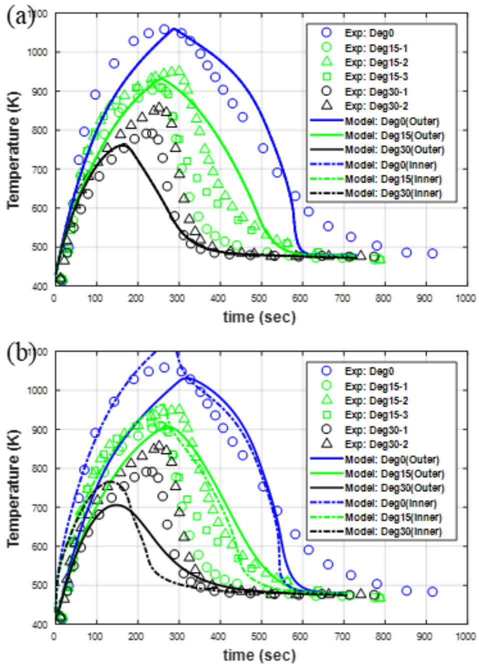

Fig. 4. Sensitivity study for dimension of the vessel (reference: LAVA-4) (a) 1D calculation (b) 2D calculation

The result of a large melt-mass case, LMP200-2, is illustrated on Fig. 5. As can be seen, there are large deviations on the experimental data although the TCs are on the same altitudinal angle from the bottom. The time at the peak temperature is comparable, but the cooling rate was under estimated. Similarly, the 15 Deg. data of LAVA-11 was under estimated. It seems that some contacts between the melt and vessel occurred on the large melt-mass experiments, LAVA-11 and LMP200-2. Thus, the heat transfer from the melt should be modified considering the some contacts at the bottom.

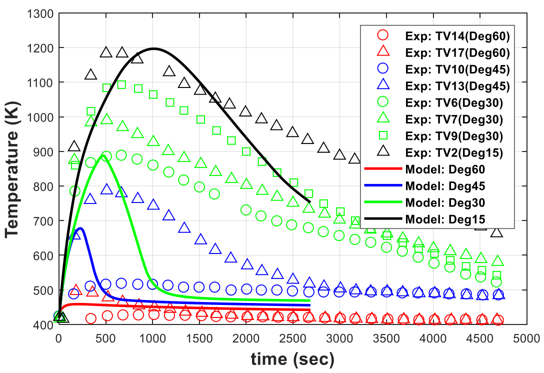

Fig. 5. Calculation results and comparison with experimental data for the large melt-mass case: LMP200-2

The comparison with other studies on gap cooling analysis is summarized on Table III.

Table III. Comparison with other codes [3-6]

	Gap formation	Water front location/ heat transfer	Dim. of melt & vessel	Ref. exp
LILAC Melt pool	~200 sec: no gap 200~ sec: 2mm gap	CCFL and heat balance/ pool boiling curve	2D melt & vessel	LAVA-4 (30kg)
CAMP	TH deformation	CCFL and heat balance/ pool boiling curve	2D melt & vessel	ALPHA-IDC001, 002 (30,50kg)
Okano study	TH Deformation	- /single HT coefficient: NB or FB	0D melt & vessel	ALPHA-IDC001,002 (30,50kg), LAVA-9 (30kg)
SAMPSON	TH Deformation	CCFL and force balance/ Monde boiling curve	2D melt & vessel	ALPHA-IDC001, 002 (30,50kg)
This study	Initial thickness: Inverse-Leidenfrost effect, Dynamics: TH fracture& deformation	CCFL and Heat balance/ Two(or three) regime model for quenching analysis	1D melt & vessel	LAVA-4 (30kg) ALPHA-IDC001, 002 (30,50kg) LAVA-11 (70kg) LMP200-2 (200kg)

ACKNOWLEDGEMENT

This work was supported by the National Research Foundation of Korea(NRF) grant funded by the Korean government(Ministry of Science and ICT) (No. NRF-2017M2B2A9072062).

REFERENCES

[1] Wolf J. R. Rempe J. L., Stickler L. A., Korth G. E., Diercks D. R., Neimark L. A., Akers D. W., Schumetz B. K., Shearer T. L., Chavez S. A., Thinnes G. L., Witt R. J., Corradini M. I., Kos J. A., 1994, TMI-2 Vessel Investigation Project Integration Report, NUREG/CR-6197

[2] Song M. W., NO H. C., 2020, Classification and Modeling of Flooding in Vertical Narrow Rectangular and Annular Channels according to Chennel-End Geometries, Nucl. Eng. Des., 110539

[3] Kim Jongtae, Kim Sang-Baik, Kim Hee-Dong, 2002, Development of LILAC-Meltpool for the Thermo-Hydraulic Analysis of Core Melt Relocated in a Reactor Vessel, KAERI/TR-2126/2002

[4] Maruyama Yu, Moriyama Kiyofumi, Nakamura Hideo, Hirano Masashi, Nakajima Kengo, 2003, Modeling for Evaluation of Debris Coolability in Lower Plenum of Reactor Pressure Vessel, J. Nucl. Sci. Tech., 40, 1, 12-21

[5] Okano Yukimitsu, Nagae Takashi, Murase Michio, 2005, Modeling and Validation of In-Vessel Debris Cooling during LWR Severe Accident, J. Nucl. Sci. Tech., 42, 4, 351-361

[6] Baglietto Emilio, Ninokata Hisashi, Naitoh Masanori, 2008, Investigation of ALPHA Experiment by Severe Accident Analysis Code SAMPSON, Nucl. Eng. Des. 238, 1561-1568